

Detecting Dynamic Community Structure in Functional Brain Networks Across Individuals: A Multilayer Approach

Chee-Ming Ting*, S. Balqis Samdin, Meini Tang, and Hernando Ombao

Abstract—Objective: We present a unified statistical framework for characterizing community structure of brain functional networks that captures variation across individuals and evolution over time. Existing methods for community detection focus only on single-subject analysis of dynamic networks; while recent extensions to multiple-subjects analysis are limited to static networks. **Method:** To overcome these limitations, we propose a multi-subject, Markov-switching stochastic block model (MSS-SBM) to identify state-related changes in brain community organization over a group of individuals. We first formulate a multilayer extension of SBM to describe the time-dependent, multi-subject brain networks. We develop a novel procedure for fitting the multilayer SBM that builds on multislice modularity maximization which can uncover a common community partition of all layers (subjects) simultaneously. By augmenting with a dynamic Markov switching process, our proposed method is able to capture a set of distinct, recurring temporal states with respect to inter-community interactions over subjects and the change points between them. **Results:** Simulation shows accurate community recovery and tracking of dynamic community regimes over multilayer networks by the MSS-SBM. Application to task fMRI reveals meaningful non-assortative brain community motifs, e.g., core-periphery structure at the group level, that are associated with language comprehension and motor functions suggesting their putative role in complex information integration. Our approach detected dynamic reconfiguration of modular connectivity elicited by varying task demands and identified unique profiles of intra and inter-community connectivity across different task conditions. **Conclusion:** The proposed multilayer network representation provides a principled way of detecting synchronous, dynamic modularity in brain networks across subjects.

Index Terms—Dynamic functional connectivity, community detection, stochastic blockmodel, Markov-switching model, fMRI.

I. INTRODUCTION

Functional architecture of the brain can be characterized as a network of interconnected regions. Study of human brain networks using neuroimaging data has offered new insights on human behavior and neurodegenerative diseases [1]. Early studies of functional magnetic resonance imaging (fMRI) assume a static functional connectivity (FC) pattern over time. Recent evidence suggests temporal dynamics of FC patterns over multiple time scales during task performance and rest [2], [3]. Dynamic FC has also been studied to examine the normal

and pathological brain connectivity patterns [4], [5]. Despite dynamic fluctuation over time, FC tends to be temporally clustered into a finite number of putative connectivity states, i.e., distinct connectivity patterns that transiently recurs over the course of experiment [6], [7]. Most studies of dynamic connectivity states focused on transition between whole-brain connectivity profiles only in terms of connectivity edges. However, switching in the topological properties of brain functional networks such as the modular or community structure has received less attention. Our goal is to develop a novel approach to quantifying dynamic FC, specifically the state-driven changes in community organization of brain networks, while also taking into account variation across individuals.

Evidence from neuroimaging studies suggest complex community structure of both structural and functional brain networks [8], where brain network can be decomposed into clusters of densely inter-connected nodes (called modules or communities) that are relatively sparsely connected with nodes in other modules. These topological modules often correspond to groups of anatomically neighboring and/or functionally-related brain regions that engage in specialized information processing. Many data-driven community detection methods have been applied to identify latent community structure in brain networks. The most widely-used approach is the modularity maximization which partitions network's nodes into non-overlapping communities that are more internally dense than would be expected by chance, by maximizing an objective function of modularity [9]. There are many computationally-efficient heuristics that search for the approximate optimal modularity [10]. Among them is the popular Louvain algorithm which is the fastest community detection methods in practice [11] but is only suited for analysis of single-layer networks, e.g., for individual subjects.

We consider a statistically-principled approach using the stochastic block model (SBM), a generative model for networks with community structure [12]. The SBM partitions a network into 'blocks' or communities of nodes according such that the probability of forming a connectivity edge between a pair of nodes depends only on which communities these nodes belong. One advantage of SBM is that it offers a richer class of community structures beyond the traditional assortative community with internally dense and externally sparse connections (i.e., the probability of an edge between nodes is higher within a community than between communities). These non-assortative structures include the core-periphery, disassortative and mixed motifs [13]. The maximizers of Newman-

C-M Ting is with the School of Biomedical Engineering & Health Science, Universiti Teknologi Malaysia, 81310 Skudai, Johor, Malaysia, and also the Biostatistics Group, King Abdullah University of Science and Technology, Thuwal 23955, Saudi Arabia (e-mail: cmting@utm.my).

S. B. Samdin, M. Tang & H. Ombao are with the Biostatistics Group, King Abdullah University of Science & Technology, Thuwal 23955, Saudi Arabia.

Girvan modularity [9] have been proven as asymptotically consistent estimators of block partitions under the SBM [14], and recently extended to degree-corrected SBM [15].

Despite that community detection has become important for brain network analysis, there has not been much progress in (1) quantifying dynamic changes in community structure over time, and (2) detecting and mapping communities across subjects. Modularity in functional networks can exhibit changes across time, e.g., over the course of task performance and learning [16], [17]. Most studies using SBMs for brain networks focused mainly on the static descriptions of functional brain modules [13], [18]. Extensions of SBM for static networks to dynamic settings have been introduced recently to detect temporal evolution of communities in social networks [19], [20]. To our knowledge, application of dynamic SBMs to time-varying brain networks is still very limited. Detecting brain community structure across subjects was traditionally performed based on individual subjects or group-averaged network. This approach however suffers from inconsistent mapping of community labels across subjects and relies on some ad-hoc template-matching techniques to register the subject-specific communities to a common template [21].

A recent solution to these problems is the multilayer network representation via aggregating multiple instances of a single network (layers) and then identifying communities across layers by maximizing a multilayer modularity function [22]. A few studies have applied this approach to time-varying brain networks to track changes in community assignments of nodes across time [16], [17], where each layer represents a snapshot of functional network at a particular time window with inter-layered couplings to connect nodes of networks between adjacent time points. It was recently modified to characterize modularity in brain networks across subjects [23]. By applying modularity maximization to a multilayer stack of individual subjects' connectivity matrices, it can find communities in all layers (i.e. subjects) simultaneously. One advantage is that it preserves community labels that are consistent across different subjects, thus allowing straightforward inter-subject mapping of community assignments.

In this paper, we extend the SBM to dynamic, multi-subject networks and adopt the multilayer modularity for detecting communities. Specifically, we develop a novel framework based on multi-subject, Markov-switching SBM (MSS-SBM) to identify dynamic changes in modular organization of brain networks across subjects. We first formulate a multilayer SBM to characterize community structure in multi-subject, time-varying brain functional networks. We leverage on the multilayer modularity maximization to find shared community partition across subjects. Secondly, we aim to detect state-based changes in the network modular organization, i.e., distinct patterns of inter-modular connectivity that repetitively occur over time and across subjects, driven by some latent brain states in response to changes in task conditions or stimuli over course of experiments. By combining the multilayer SBM and a hidden Markov model (HMM) to describe the evolution of the underlying states, the proposed MSS-SBM is able to estimate simultaneously the change-points of time-evolving modularity states and the block structure in each state, i.e.,

intra- and inter-modular connections. It is flexible to capture a variety of dynamics, e.g., a shift from a connectivity state which is highly modular to a state which is less modular and more integrated throughout the network. Moreover, our model does not require for the timing of the switching between states to be known apriori. In contrast to a similar setup in [24] that uses hidden-Markov SBM on the observed time-varying graphs directly, our approach has the advantage of identifying distinct temporal states in dynamic community structure based on lower-dimensional, time-evolving inter-modular connectivity matrices. Moreover, [24] only analyzed the group-averaged dynamic functional networks and ignores the variation across subjects. A multi-subject SBM based on mixture modeling and variational Bayesian estimation was recently proposed by [25], which however did not address the dynamic nature of the community organization. Our earlier work [26] proposed a Markov-switching SBM which revealed alternating modular structure in fMRI functional networks during language processing, but it uses spectral clustering for community detection and is limited to single-subject analysis. We apply the proposed MSS-SBM to task fMRI data in Human Connectome Project (HCP) to study rapid switching of brain network modularity evoked by repetitive tasks.

The main contributions of this work are as follows:

- 1) We propose a novel framework based on MSS-SBM to characterize state-based dynamic community structure of brain functional networks across subjects.
- 2) Our method combines a multi-subject, time-varying SBM with an HMM to identify distinct repeating states in the time-varying inter-community connectivity without a priori knowledge about the timing of the structural switching between these states of network modularity.
- 3) To the best of our knowledge, our proposed approach is the first that leverages on the multilayer modularity maximization to detect community structure of brain networks in multiple subjects simultaneously under the proposed MSS-SBM. Given the common community partition with consistent mapping of nodes' community assignments across subjects, it allows us to identify a set of group-level connectivity states.

II. MODELING MULTI-SUBJECT DYNAMIC COMMUNITY STRUCTURE IN BRAIN NETWORKS

We first describe a novel multilayer SBM for modeling community structure in multi-subject, time-varying brain functional networks. To identify state-related changes in the time-evolving community structure, we further develop a MSS-SBM that combines the multilayer SBM with an HMM to describe the switching between distinct states of modular connectivity patterns over time and across subjects.

A. Multilayer SBM

We consider a collection of undirected graphs of multi-subject, time-varying functional brain networks $\mathcal{G} = \{G^{r,t}, t = 1, \dots, T, r = 1, \dots, R\}$ that shares a set of nodes $V \equiv \{V_1, \dots, V_N\}$ (voxels or regions of interest (ROIs)) over T time points for a group of R subjects. We can view \mathcal{G} as a doubly-indexed multilayer networks where each (r, t) -th layer

$G^{r,t} \equiv \{V, E^{r,t}\}$ represents a snapshot of a network observed at time step t for the r -th subject, with a set of (possibly time-changing) connectivity edges between N individual nodes denoted by $E^{r,t} \equiv \{e_{ij}^{r,t}, 1 \leq i, j \leq N\}$. We assume the number of brain nodes $N = |V|$ to be fixed over time and subjects. We define the corresponding adjacency (or connectivity) matrix representations of the multi-subject, time-dependent networks in \mathcal{G} by $\mathbf{W} = \{\mathbf{W}^{r,t}, t = 1, \dots, T, r = 1, \dots, R\}$ where $\mathbf{W}^{r,t} = [w_{ij}^{r,t}]$ is a $N \times N$ symmetric matrix at time t for subject r with $w_{ij}^{r,t} = 1$ if there exists a connecting edge between the nodes i and j , $e_{ij}^{r,t} \in E^{r,t}$ and $w_{ij}^{r,t} = 0$ otherwise. We assume there is no self-edge, i.e., $w_{ii}^{r,t} = 0$. The time-varying adjacency matrices for each subject were estimated by thresholding sliding-window correlation matrices computed over shifted windowed segments of fMRI time series. The threshold is selected to achieve a targeted density of edges in the adjacency matrices, defined for undirected graph as $\kappa = 2\epsilon_\tau/N(N-1)$, $\kappa \in (0, 1)$ where ϵ_τ is the number of edges preserved at some threshold τ [27].

Under multilayer SBM, functional networks in \mathcal{G} are assumed to be generated from a set of SBMs, where $\mathbf{W}^{r,t}$ of individual layers follows a regular single-layer SBM which partitions the N network nodes into K blocks or communities (clusters of anatomically or functionally-related brain regions). Let $\mathbf{g} = \{g_1, \dots, g_N\}$ be community membership vector for N nodes, where $g_i \in \{1, \dots, K\}$ indicates the community membership label of node V_i and $g_i = k$ if node V_i belongs to community k . We also denote $\Gamma_k = \Gamma_k(\mathbf{g}) = \{V_i : g_i = k\}$ and $N_k = |\Gamma_k|$ to be the set of nodes and number of nodes within community k for $k = 1, \dots, K$. We can rewrite in a $N \times K$ membership matrix $\Omega = [\omega_{ik}]$ such that i -th row of Ω is 1 in column g_i , $\omega_{i,g_i} = 1$ and 0 elsewhere. Each node belongs only to one community (i.e., the communities or blocks are disjoint) such that $\sum_{k=1}^K \omega_{ik} = 1$. Conditioned on the community assignments of nodes g_i and g_j , edges within each individual network layer (r, t) are generated independently according to a Bernoulli distribution

$$w_{ij}^{r,t} \sim \text{Bernoulli}(\theta_{g_i g_j}^{r,t}) \quad (1)$$

where $\theta_{kl}^{r,t} \in [0, 1]$ is the probability of edges existing between any node in community k and any node in community l at time t for subject r . In other words, probability of connection between two nodes depends only on the community blocks to which these nodes belong. We then define a $K \times K$ symmetric modular connectivity matrix by $\Theta^{r,t} = [\theta_{kl}^{r,t}]$ whose diagonal elements $\theta_{kk}^{r,t}$ and the off-diagonals $\theta_{kl}^{r,t}, k \neq l$ captures the within-module and between-module connectivity, respectively. The set of parameters of the multilayer SBM is denoted by $\{\Omega, \Theta\}$ with $\Theta = \{\Theta^{r,t}; t = 1, \dots, T, r = 1, \dots, R\}$. Note that we assume the network community partition as defined by Ω to be shared by all subjects and constant over time, but the modular connection probability matrix $\Theta^{r,t}$ is allowed to evolve across time and to vary across subjects. We consider estimation of multilayer SBM with K blocks in the *a posteriori* setting where both the community membership labels Ω and the connectivity matrices Θ are both unknown and to be estimated.

B. Multi-Subject Markov-Switching SBM

In contrast to recent studies of dynamic connectivity states in the whole-brain connectivity edges [7], [28]–[30], our goal in this paper is to identify distinct states in the time-evolving modular organization of networks and the temporal locations of transitions between states. We develop a regime-switching SBM to characterize changes the inter-community connectivity driven by a set of recurring latent states over time and subjects. In particular, let $\beta^{r,t} = \text{vec}(g(\Theta^{r,t}))$ be K^2 -dimensional vectorized version of $g(\Theta^{r,t})$ and $g(\Theta^{r,t}) = \text{logit}(\Theta^{r,t})$ whose elements are logit of $\theta_{kl}^{r,t}$, $\text{logit}(\theta_{kl}^{r,t}) = \log(\theta_{kl}^{r,t}) - \log(1 - \theta_{kl}^{r,t})$. We assume the logit transform of time-varying module connection probabilities $\Theta^{r,t}$ in (1) to follow an HMM

$$s_{r,t} | s_{r,t-1} = \ell \sim \text{Multi}(\pi_{\ell 1}, \dots, \pi_{\ell S}) \quad (2)$$

$$\beta^{r,t} | s_{r,t} = m \sim N(\mu_{\Theta}^{[m]}, \Sigma_{\Theta}^{[m]}) \quad (3)$$

$$\mathbf{W}^{r,t} \sim \text{Bernoulli}(\Theta^{r,t}) \quad (4)$$

where $s_{r,t} \in \{1, \dots, S\}$ for $t = 1, \dots, T$ is a sequence of state variables which varies over time for k -th subject, S is the number of states. The variation in the modular connectivity structure over time and subjects is determined by the latent state indicator $s_{r,t}$ which follows a Markov process with $K \times K$ transition matrix $\Pi = [\pi_{\ell m}]_{1 \leq \ell, m \leq S}$, where $\pi_{\ell m} = P(s_{r,t} = m | s_{r,t-1} = \ell)$ is the probability of transition from state ℓ at time $t-1$ to state m at time t . The parameters $\mu_{\Theta}^{[m]}$ and $\Sigma_{\Theta}^{[m]}$ capture respectively the mean and variations of inter-modular connection probabilities in each state $m = 1, \dots, S$. In analyzing group-wise time-varying networks averaged over subjects, [24] fitted the hidden Markov SBM directly on the high-dimensional $N \times N$ node-wise connectivity matrices \mathbf{W}^t , specifying the evolution of connectivity parameters $\Theta^{[s_t]}$ as a piecewise constant function of s_t . In contrast, the advantage of our approach is that it utilizes the HMM for $K \times K$ modular connectivity matrices $\Theta^{r,t}$, which involves a smaller number of parameters in the state estimation and thus improving computational and statistical efficiency. Moreover, it allows clustering of the time-evolving community structure into states that maybe associated with different tasks and conditions over the time course of experiment. Given the model (2)-(4), the aims are to estimate the state sequence $s_{r,t}$ which indicates which regime to be most likely active at each time point and for each subject, and the state-specific modular connectivity parameters $\{\mu_{\Theta}^{[m]}, \Sigma_{\Theta}^{[m]}, m = 1, \dots, S\}$.

III. ESTIMATION

We develop a two-stage estimation procedure for the proposed MSS-SBM to identify state-based dynamic community structure in multiple subjects.

Stage 1: Fit the multilayer SBM to the multi-subject, time-varying adjacency matrices in \mathbf{W} . We first estimate the common block structure Ω , by applying the modularity maximization algorithm to a group-level multilayer network object comprising single networks of individual subjects to uncover the shared nodes community memberships \mathbf{g} over all subjects simultaneously. Given the estimated community partition, we then estimate by maximum likelihood (ML)

method the inter-modular connection probabilities $\{\Theta^{r,t}\}$ for each subject and each time point based on $\{\mathbf{W}^{r,t}\}$.

Stage 2: Fit the HMM on concatenated $\{\Theta^{r,t}\}$ to identify dynamic community states. This step produces an estimate of change-points between states across time and subjects via the mostly likely state sequence $s_{r,t}$ and the state-specific module connectivity parameters $\{\mu_{\Theta}^{[l]}, \Sigma_{\Theta}^{[l]}\}$.

A. Community Detection

To detect communities in multi-subject brain functional networks, we develop a method inspired by the modularity maximization (Q_{\max}) approach for estimating the multilayer SBM. The Q_{\max} algorithm provides an estimate of the number of communities K which is then used for fitting the SBM. We use the single-layer generalized Louvain algorithm to estimate the community membership of nodes \mathbf{g} at the individual subject level, and develop an extension of the Q_{\max} to multilayer networks for group-level analysis.

1) *Single-Layer Modularity Maximization:* Let $\bar{\mathbf{W}}^r = [\bar{w}_{ij}^r]$ be the adjacency matrix for subject $r = 1, \dots, R$ which is obtained by thresholding the time-averaged correlation matrix. For single-subject community detection, we aim to find the optimal community membership vector $\mathbf{g}_r = \{g_{1r}, \dots, g_{Nr}\}$ for each subject r independently. This can be accomplished by maximizing a modularity quality function [31] of single-layer network, defined for each subject as

$$Q(\mathbf{g}_r) = \sum_{i,j} (\bar{w}_{ij}^r - p_{ijr}) \delta(g_{ir}, g_{jr}) \quad (5)$$

where $p_{ijr} = \frac{\kappa_{ir}\kappa_{jr}}{2L_r}$ denotes the expected weight of the edges connecting nodes i and j under the Newman-Girvan null model, $\kappa_{ir} = \sum_j \bar{w}_{ij}^r$ is the degree of node i , L_r is total number of edges in the network of subject r , and $\delta(g_{ir}, g_{jr}) = 1$ if nodes i and j belong to the same community, and 0 otherwise. Then, the modularity maximization estimator of the community partition is defined by $\hat{\mathbf{g}}_r = \operatorname{argmax}_{\mathbf{g}_r} Q(\mathbf{g}_r)$. The partition that gives the greatest value of Q is considered as a good estimate of a network's community structure. We will drop the subject index r for notational brevity.

To solve the single-subject or single-layer Q_{\max} , we employ the Louvain algorithm which is simple and computationally-efficient. This community detection algorithm aims to find communities in a network assuming that connectivity between nodes within communities is stronger than connectivity between nodes across communities. It is a two-step iterative algorithm. As initialization each node in the network is its own community. In first step, each node will be assigned to a community of neighboring nodes if the resulting network modularity Q is maximized. The gain in modularity ΔQ by moving a node i into community k is given by [11]

$$\Delta Q = \left[\frac{\Sigma_{in} + \kappa_{i, \text{in}}}{2L} - \left(\frac{\Sigma_{\text{tot}} + \kappa_i}{2L} \right)^2 \right] - \left[\frac{\Sigma_{in}}{2L} - \left(\frac{\Sigma_{\text{tot}}}{2L} \right)^2 - \left(\frac{\kappa_i}{2L} \right)^2 \right] \quad (6)$$

where $\Sigma_{in} = \sum_{ij \in \Gamma_k} \bar{w}_{ij}$ is the number of edges within community k , $\Sigma_{\text{tot}} = \sum_{i \in \Gamma_k} \kappa_i$ is the total number of edges

incident to nodes of community k , κ_i is the degree of node i and $\kappa_{i, \text{in}} = \sum_{j \in \Gamma_k} \bar{w}_{ij}$ is number of edges from node i to other nodes in the community k . The second step involves constructing a network with the new community structure detected in first step. The two steps are repeated iteratively until convergence of the network modularity.

2) *Multilayer Modularity Maximization:* We apply the multilayer modularity approach [22] for community detection in the multi-subject networks to find a group-level community partition. With multilayer modularity optimization, one can study the dynamic network organization over a set of temporally-linked time-dependent networks [8], [13], [32], [33]. This method will identify the nodes community memberships of the functional connectivity networks for all subject simultaneously. The advantage of this approach is that it can determine consistent community labels for all nodes in multi-subject networks. In contrast, conventional single-layer community detection methods such as spectral clustering suffer from problem of arbitrary community label switching and hence inconsistent mapping of nodes assignments across different subjects [20], [34], [35].

Let $\bar{\mathbf{W}} = \{\bar{\mathbf{W}}^1, \dots, \bar{\mathbf{W}}^R\}$ be the set of R subject-specific adjacency matrices observed for a multilayer network where each layer represents a static functional brain network of a particular subject. The multilayer modularity across all pairs of subjects r and s is written as

$$Q_{MS} = \frac{1}{2\mu} \sum_{ijrs} [(\bar{w}_{ij}^r - \gamma_r p_{ijr}) \delta(g_{ir}, g_{jr}) + \delta(i, j) C_{jrs}] \delta(g_{ir}, g_{js}) \quad (7)$$

where g_{ir} is the community assignment of node i in layer r , $\delta(g_{ir}, g_{js}) = 1$ indicates that community assignments g_{ir} and g_{js} are identical, and $p_{ijr} = \frac{\kappa_{ir}\kappa_{jr}}{2L_r}$ is the expected weight of edges within layer r . The total number of edges in the adjacency tensor $\bar{\mathbf{W}}$ is $\mu = 0.5 \sum_{js} (\kappa_{js} + c_{js})$ where $c_{js} = \sum_r C_{jrs}$ is the interlayer strength of node j in layer s . This modularity optimization depends on intra-layer structural resolution γ and interlayer coupling parameter between layers r and s of the same nodes j , C_{jrs} . By adding interlayer connections of weight C , optimization of (7) yields community labels that are preserved across subjects. We used all-to-all interlayer coupling since the network layers across subjects do not reflect specific order [22]. Larger values of γ results in many small communities while large values of C produce communities that are common across subjects.

B. Estimation of Modular Connectivity Parameters

Given the estimated community partition, we can estimate the subject-specific, time-dependent modular connectivity parameters $\{\Theta^{r,t}\}$ via maximum likelihood. For any nodes community assignments \mathbf{g} , the log likelihood of a set of $R \times T$ adjacency matrices \mathbf{W} under the multilayer SBM is

$$f(\mathbf{W}|\Theta, \mathbf{g}) = \sum_{r=1}^R \sum_{t=1}^T \sum_{i < j} \left\{ w_{ij}^{r,t} \log \theta_{g_i, g_j}^{r,t} + (1 - w_{ij}^{r,t}) \log(1 - \theta_{g_i, g_j}^{r,t}) \right\}. \quad (8)$$

Given the estimated $\hat{\mathbf{g}}$, let $\hat{N}_k = |\Gamma_k(\hat{\mathbf{g}})| = |\{V_i : \hat{g}_i = k\}|$ denote the number of nodes assigned to community k , and n_{kl} be the number of possible edges between communities k and l , i.e., $n_{kl} = \hat{N}_k \hat{N}_l$ for $k \neq l$ and $n_{kk} = \hat{N}_k(\hat{N}_k - 1)$. The ML estimate of the connectivity parameters Θ is

$$\hat{\theta}_{k,l}^{r,t} = \frac{1}{n_{kl}} \sum_{i < j} w_{ij}^{r,t} 1\{\hat{g}_i = k, \hat{g}_j = l\},$$

$$t = 1, \dots, T, \quad r = 1, \dots, R, \quad k, l = 1, \dots, K \quad (9)$$

where $1\{\cdot\}$ is the indicator function. The estimated inter-block connection probabilities $\hat{\theta}_{k,l}^{r,t}$ correspond to ratios of number of observed edges relative to possible edges within each block, which is called as block densities.

C. Identification of Dynamic Community States

We fit an HMM in (2)-(3) on the estimates $\hat{\Theta} = \{\hat{\Theta}^{r,t}; t = 1, \dots, T, r = 1, \dots, R\}$ to identify the distinct, recurring states in the time-evolving inter-modular connectivity that are common across subjects. The timing of shifts between states and the modular connectivity pattern in each state can be estimated simultaneously. Let $(\hat{\beta}^{1,1}, \hat{\beta}^{1,2}, \dots, \hat{\beta}^{R,T})$ be a set of RT concatenated vectors of the logit of estimated time-varying modular connection probabilities over all subjects. Given a set of HMM parameters $\lambda = \{\mathbf{\Pi}, \mu_{\Theta}^{[m]}, \Sigma_{\Theta}^{[m]}\}$, the temporal dynamics of the states over subjects $\{s_{r,t}\}$ can be obtained by extracting the most likely state sequence using the Viterbi algorithm

$$\hat{s}_{1,1}, \dots, \hat{s}_{R,T} = \underset{s_{1,1}, \dots, s_{R,T}}{\operatorname{argmax}} p(s_{1,1}, \dots, s_{R,T}, \hat{\beta}^{1,1}, \dots, \hat{\beta}^{R,T} | \lambda). \quad (10)$$

The estimators for the state-specific block connectivity parameters $\{\mu_{\Theta}^{[m]}, \Sigma_{\Theta}^{[m]}\}$ can be computed iteratively using the Baum-Welch algorithm. See [36] for details of HMM estimation.

IV. SIMULATIONS

In this section, we shall evaluate the performance of our method on synthetic multi-subject networks.

1) *Community Recovery*: In this simulation, we first access the performance of different community detection methods in recovering a consensus community partition that is shared across different subjects. We generate binary networks of R subjects from the multilayer SBM with balanced community size (with N nodes equally partitioned into K communities). The true community labels of nodes \mathbf{g} are fixed and common across subjects. The modular connectivity matrix is set using the parameterization in [35]

$$\Theta = \alpha \Theta_0 : \quad \Theta_0 = \lambda \mathbf{I}_K + (1 - \lambda) \mathbf{1}_K \mathbf{1}_K^T, \quad 0 < \lambda < 1 \quad (11)$$

where \mathbf{I}_K is the $K \times K$ identity matrix and $\mathbf{1}_K$ is the $K \times 1$ vector of 1's. The quantity λ reflects the relative difference of the within- and between-community edge probabilities. The network sparsity is controlled by α , where $N\alpha$ provides an upper bound on the average expected node degree. It is more difficult to recover the communities when α and λ are close to 0. We also allows inter-subject variability in the connectivity

matrix by adding some subject-specific random deviations such that $\Theta^r = \Theta + \epsilon_r \mathbf{I}_K$ with $\epsilon_r \sim U[-0.1, 0.1]$.

We compare the performance of the proposed multilayer modularity maximization (Q_{\max}) algorithm with two single-layer methods: (1) Spectral clustering which performs K-means clustering on the K leading eigenvectors of the graph Laplacian [34], and (2) Single-layer Q_{\max} using the Louvain algorithm (in Section III.A.(1)) as baseline. Both competing methods are widely used for community recovery with promising empirical performance, and have been shown to enjoy good statistical guarantee under the SBM [35], [37]. Note that the number of communities K was assumed known for the spectral clustering, and estimated from the simulated data for the Q_{\max} methods. We measure the performance of all methods by the adjusted Rand index (ARI) between the ground-truth community labels \mathbf{g} and its estimates $\hat{\mathbf{g}}$. The ARI is a measure of similarity between two partitions, taking values between 0 (random label assignments) and 1 (perfect recovery of true partition).

Fig. 1 shows the performance comparison, in terms of ARIs over individual subjects, under different scenarios: increasing number of nodes N , number of subjects R , number of communities K and varying levels of network sparsity α . From Fig. 1(a), we see that the multilayer Q_{\max} clearly outperforms the single-layer methods, achieving perfect recovery even when the number of nodes per community is very small. This suggests the robustness of the multilayer Q_{\max} in small sample settings due to the pooling of data across multiple layers to estimate the common community structure accurately. The performance of both single-layer methods improves steadily as N increases, with the single-layer Q_{\max} reaching ARI of close to 1 faster than the spectral clustering. Fig. 1(b) shows that small number of layers/subjects ($R = 20$) is sufficient for the multilayer Q_{\max} to yield an exact community reconstruction. The single-layer methods have slightly lower accuracy of community detection and do not show any improvement with more layers because they carry out the community detection in individual networks independently. Fig. 1(c) shows that the multilayer Q_{\max} is able to consistently recover the communities for large number of communities. The ARI of both single-layer methods drops with increasing K , at a much faster rate for the spectral clustering compared to the single-layer Q_{\max} . In Fig. 1(d), the single-layer methods especially the spectral clustering perform poorly when the network is sparse (low values of α). This agrees with other studies which have shown that spectral methods tend to suffer from inconsistency in sparse graphs [38]. As expected, the accuracy of these methods increases when the networks become denser as α increases. In contrast, the multilayer Q_{\max} remains robust even in the sparse network case.

2) *Estimation of State-Related Changes*: We further evaluate the proposed MSS-SBM in identifying underlying temporal regime changes in the modular connectivity patterns. We generated time series of synthetic dynamic functional networks for a cohort of R subjects, according to the time-varying, multi-subject SBM of (1). To emulate the hidden dynamics of regime switching in the network community structure, the simulated sequences of $T = 240$ temporal graphs $\{\mathbf{W}^{r,t}\}$

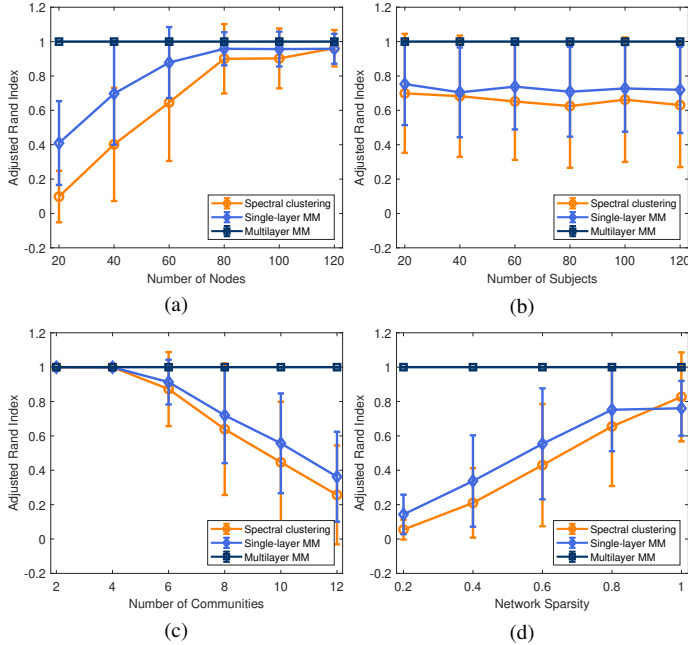


Fig. 1. Performance comparison of various methods for community detection in multisubject networks as measured by ARI between ground-truth and estimated community labels for four simulation settings. (a) Number of nodes N increases, $K = 5$, $R = 100$, $\alpha = 0.8$. (b) Number of subjects R increases, $N = 120$, $K = 8$, $\alpha = 0.8$. (c) Number of communities K increases, $N = 120$, $R = 100$, $\alpha = 0.8$. (d) Different levels of network sparsity α , $N = 120$, $K = 8$ and $R = 100$. Lines and error bars represent mean and standard deviations over subjects.

were characterized by time-evolving modular connectivity $\Theta^{[s_t]}$ driven by underlying piece-wise stationary state time course $s_t \in 1, \dots, S$. Here we drop the subject index r in s_t assuming all subjects to share identical state dynamics. To imitate the typical block-design paradigm in task-based fMRI experiment, time-blocks of states (each state represents a task or stimulus) were interleaved and repeated over the time course. This reproduces quasi-stable, recurring network modular structure over time points. We consider $S = 3$ distinct states each has a unique modular connection probability matrix $\Theta^{[m]}$ of the form (11) with $\lambda = 0.9$ for $m = 1$, $\lambda = 0.75$ for $m = 2$ and $\lambda = 0.6$ for $m = 3$, which represent states of high, medium, and low within-community connectivity, respectively. We further introduce temporal variability by adding random fluctuations into the piecewise constant trajectory $\Theta^{[s_t]}$, i.e., $\beta^t = \beta^{[s_t]} + \eta^t$, $\eta^t \sim N(\mathbf{0}, \sigma \mathbf{I})$ where $\beta^{[s_t]} = \text{vec}(g(\Theta^{[s_t]}))$. The estimates of state sequence \hat{s}_t is obtained via Viterbi algorithm (10), and the state-specific connectivity parameters $\hat{\Theta}^{[m]} = E[\Theta^t | S_t = m]$ from the inverse logit of the estimated means of HMM Gaussian observation density $g^{-1}(\hat{\mu}_{\Theta}^{[m]})$.

To measure dynamic state estimation performance, we compute the ARI between the true and estimated partitions of the T temporal observations into states based on \hat{s}_t . It is defined in terms of numbers of pairs of time points that are correctly identified as belonging to the same or different states, where $\text{ARI} = 1$ indicates perfect recovery of the true state sequence. This measure also indirectly evaluates the change-point detection in the modular connectivity structure. We also calculate the mean squared error between the ground-truth and estimated time-evolving modular connectivity matrices over

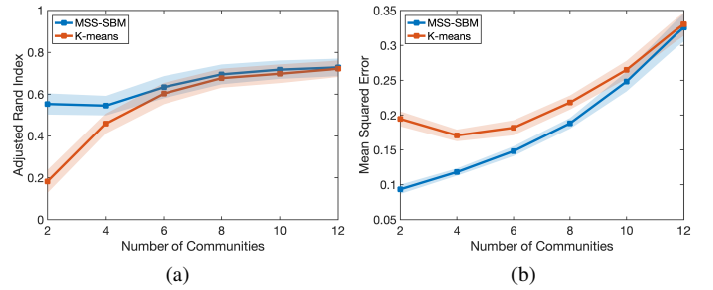


Fig. 2. Performance of MSS-SBM and K-means clustering in estimating state-based dynamic inter-modular connectivity in simulated multi-subject networks for increased number of communities K with $N = 120$, $T = 240$ and $S = 3$. (a) ARI of dynamic state identification. (b) MSE for estimated time-dependent connectivity matrices. The intervals represent standard deviations over $R = 50$ subjects and 100 replications of simulation for each subject.

the time course, $\text{MSE} = T^{-1} \sum_{t=1}^T \|\hat{\Theta}^{[s_t]} - \Theta^{[s_t]}\|_F^2$ where $\|\mathbf{H}\|_F = \text{tr}(\mathbf{H}'\mathbf{H})^{1/2}$ denotes Frobenius norm of matrix \mathbf{H} .

We assess the scalability of MSS-SBM for dynamic connectivity estimation in the presence of large number of communities K . Fig. 2 plots the ARIs and MSEs over $R = 50$ subjects as a function of increasing K with fixed $N = 120$. Compared to the K-means clustering approach which is widely used in estimating dynamic brain connectivity states, the MSS-SBM perform better in both tracking of dynamic regimes and connectivity estimation, particularly when K is small. This implies the advantages of using Markov process in the MSS-SBM to model the temporal evolution of the connectivity states, and the Gaussian observation density to account for variations within each state. Fig. 2(a) shows improved accuracy of dynamic regime identification with increasing K . This is because larger K may provide more information about the distinct inter-community connectivity structure that allows better discrimination between different temporal states. Despite improved temporal state partitioning, estimation errors of connectivity matrices drop, as shown in Fig. 2(b). This is due to the larger dimension of the state-specific modular connectivity matrices when K increases, which are poorly estimated given fixed sample size available for each state.

V. APPLICATION TO TASK fMRI

We apply the proposed MSS-SBM approach to identify state-driven dynamic switching in community structure of fMRI functional networks across subjects. We assume there is a common community partition across subjects and time, but allow the inter-modular connectivity to vary as evoked by alternating conditions over the time course of experiment. The number of connectivity states corresponds to the number of conditions, however the timing of changes in the connectivity states between conditions is unknown a priori. Based on adjacency matrices estimated from fMRI data, we evaluated both the subject-specific and multi-subject community detection using the single-layer and multilayer Q_{\max} algorithm, respectively. Given the community partition, time-evolving inter-modular connectivity matrices are estimated by ML followed by HMM fitting to identify the dynamic connectivity states.

A. Data & Pre-processing

We analyzed the task-related fMRI data of 400 subjects for the language and motor tasks from the Human Connectome

Project. The data were acquired with 3T Siemens Skyra with TR = 720 ms, TE = 33.1 ms, flip angle = 52°, BW = 2290 Hz/Px, in-plane FOV = 208 x 180 mm, 72 slices, 2.0 mm isotropic voxels. Refer to [39] for details of this dataset.

Language data: The experimental paradigm is block-design alternating between sentence judgments (story) and arithmetic (math) tasks [40]. Subjects were given four sets of story-math tasks with average duration of approximately 30s for each task. In the story task, subjects were given a short audio with 5-9 sentences followed by a question regarding topic of the story which required the subjects to choose an answer from two given selections. In the math task, the subjects were given a few basic arithmetic questions such as additional and subtraction and followed by answer selection for each question. Each run has $T = 316$ time scans and 8 blocks. The onset of task cues can vary across different subjects.

Motor data: The task involves execution of five motor movements: left-hand, left-foot, right-hand, right-foot and tongue movement. Each movement was repeated twice with duration of 12s with cue of 3s prior to the executions. Each dataset has a total of $T = 284$ scans, 10 task blocks and 3 fixation blocks per run. Unlike the language tasks, the onset timing of each task was identical for every subject.

Both datasets were minimally preprocessed with structural and functional HCP pre-processing pipelines version of 3.13.2 [41]. We used the automated anatomical labeling (AAL) for parcellation of the whole brain into 90 anatomical regions of interest (ROIs) and computed an averaged fMRI time series for each ROI by averaging over voxels.

B. Results for Subject-Specific Community Detection

To detect subject-specific community structure, we computed the corresponding adjacency matrices for static connectivity graphs of individual subjects by thresholding correlation matrices between pairs of ROI fMRI time series. Here, we used proportional thresholding by setting $\tau_{PT} = \kappa \times 100\%$ percentage of entries with the strongest absolute correlation values to 1 and others to zero. This technique produces a fixed density of edges in graphs across subjects and time windows, and thus enabling meaningful comparison of topological organization between different groups and conditions [42]. We varied the edge density τ_{PT} from 0% to 50% with step size of 0.1%, and computed the modularity and global efficiency indexes which quantify functional segregation and inter-modular integration of the resulting networks, respectively. We chose $\tau_{PT} = 25\%$ which gives an optimal balance between modularity and global efficiency.

Fig. 3 shows the distribution of detected number of communities by Louvain algorithm over the 400 subjects for the language and motor tasks. The averaged number of communities over subjects for the language and motor tasks are 11.51 and 12.38, respectively. The most frequent number of communities detected for both datasets is 9, and only few subjects have number of communities over 20. The results suggest the variability in number of communities across different subjects.

To obtain a consistent mapping of community partition across subjects from single-subject analysis is non-trivial since each subject has different number of communities. To solve

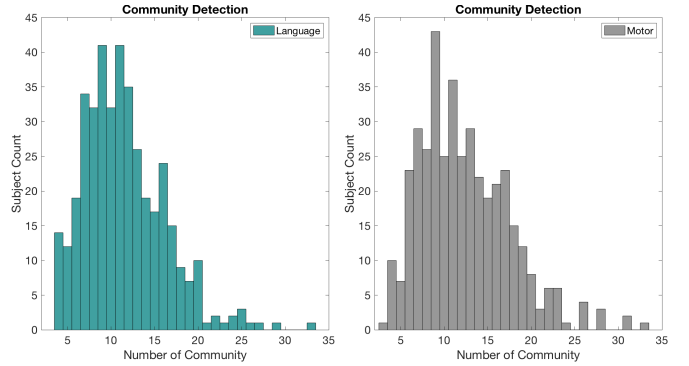


Fig. 3. Distribution of the number of detected brain communities for the language (green) and motor (grey) tasks over 400 subjects.

this, we compute a $N \times N$ community association matrix $\mathbf{P}_r = [P_{rij}]$ for each subject r , where P_{rij} is equal to 1 if nodes i and j are assigned to the same community. Fig. 4 shows the association matrices for five randomly selected subjects from both datasets. We can investigate the consensus community partition by counting occurrence over subjects that a pair of nodes belong to same community, i.e., $\mathbf{P} = \sum_{r=1}^R \mathbf{P}_r$. Fig. 5 shows the top 1% pairs of nodes that are most consistently assigned to the same community. We can see community structure for both language and motor tasks involve the frontal and thalamus areas. The motor tasks engage additional regions related to motor control and execution of voluntary movement such as precentral gyrus and rolandic operculum.

We further analyzed the regime changes in the community structure of dynamic functional networks for both the language and motor tasks using Markov-switching SBM (MS-SBM) as in [26] - a special case of MSS-SBM for single subject. The dynamic FCs were estimated based on sliding-windowed correlations with window size of 20 time points. The time-varying FC graphs were obtained by the proportional thresholding of the sliding-windowed correlation matrices. Given the estimated subject-level community membership of the 90 ROIs using Louvain algorithm, we computed the subject-specific, time-varying inter-modular connectivity parameters by ML method as in (9) and then fitted an HMM for each subject individually to detect the dynamic community regimes. The performance of Viterbi algorithm in (10) in tracking temporal regimes is compared with the K-means clustering which is widely used in dynamic connectivity state estimation.

Fig. 6 shows the tracking of dynamic regimes of the inter-modular connectivity for each subject via the estimated state sequence $\{\hat{s}_{r,t}\}$. We fitted MS-SBM with $S = 2$ and $S = 6$ states on the dynamic functional networks for the language and motor tasks, respectively. Here we assume the number of dynamic community states S corresponds to the number of tasks in the experiments. Compared to the K-means approach, the estimates by MS-SBM give a better tracking of temporal regimes changes in modular connectivity, which follow more closely the changes in the tasks (indicated as the ground-truth state sequence) over the time course of experiment for both datasets. We can see that the MS-SBM provides a more accurate detection of the abrupt change points between regimes than the K-means clustering which suffers

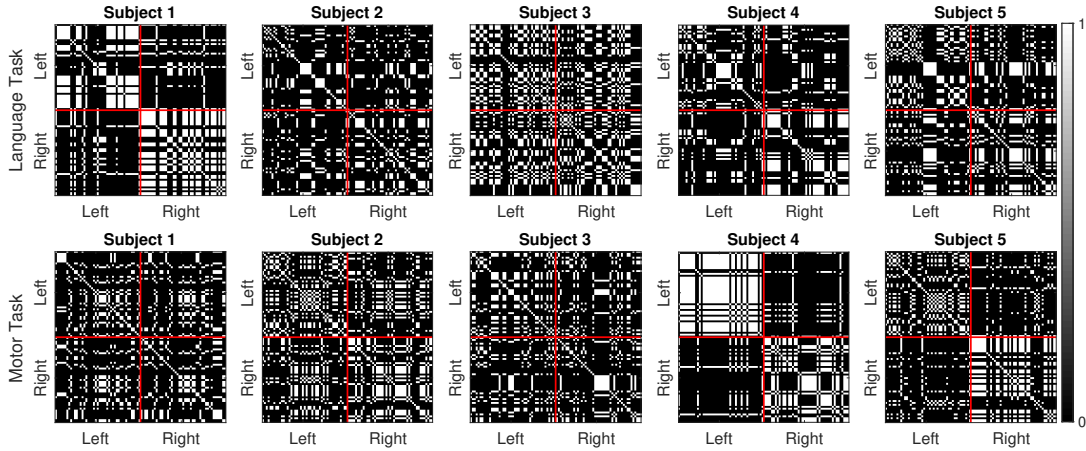


Fig. 4. Community associate matrices for 5 subjects for language task (Top) and motor task (Bottom). The ROI-wise entries in the matrices are arranged according to left and right brain hemisphere.

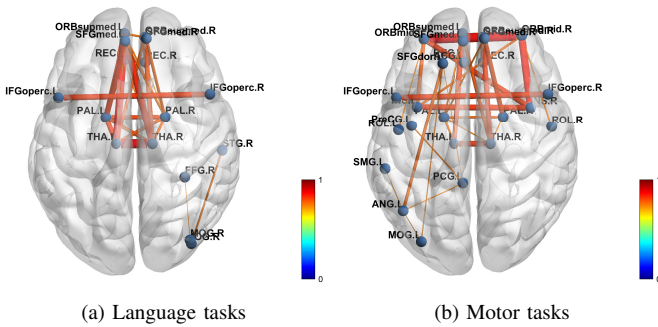


Fig. 5. Top 1% pairs of connected ROIs that are most frequently assigned to the same community over all subjects.

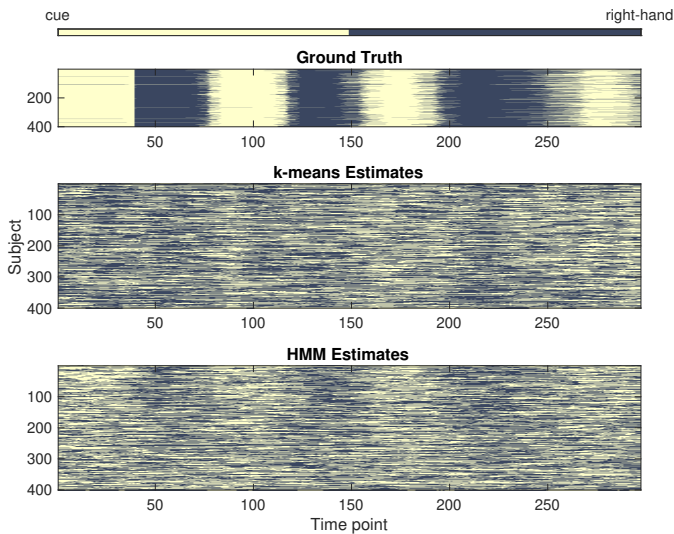
from gross change-point detection and produces spurious temporal state estimation. The state estimation by MS-SBM was accomplished in an unsupervised manner, i.e., without being pre-trained from labeled data. Despite the reasonably good estimates of the MS-SBM, the aim is not an exact recovery of task states from experimental designs but to investigate the inter-subject variability in the dynamic community structure of brain networks. We can see considerable heterogeneity in the temporal state dynamics across subjects, probably due to individual differences in the response to changes in the tasks and stimuli.

C. Results for Multi-Subject Community Detection

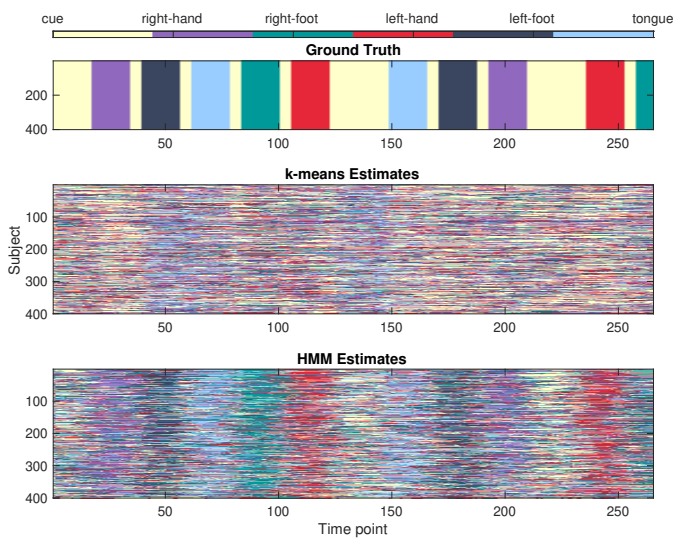
We applied the multilayer Q_{\max} approach in Section III.A.2 to identify a group-level community structure of functional networks across subjects under the proposed MSS-SBM model. We averaged the time-varying connectivity matrices for individual subjects to construct subject-specific networks, which were concatenated to form a multilayer network ensemble in which layers represent single-subject networks. The nodes' community assignment in all subjects were then estimated simultaneously by maximizing the multilayer modularity in (7) over all subjects, which was accomplished by the generalized Louvain algorithm [43]. We set $\gamma_r = \gamma = 1$ as commonly used for community detection for human brain networks [44]. To determine the interlayer connection weight, we investigated a range of values $[0.9, 1, 1.1]$, and chose

$C_{jrs} = C = 1$ which yields a consensus community partition across all subjects. Fig. 7 shows the group-level community assignment of the 90 ROIs for the language task over the 400 subjects. There are 12 communities detected, including 3 large communities (Community #1, #2 and #5), one small community (#12) and 8 singleton communities which are composed of a single node (#3, #4 and #6 - #11). Almost 90% of ROIs or nodes assigned to community #1 are located in the left hemisphere of the brain and 86% of nodes assigned to community #2 in the right hemisphere. This is consistent with the well-established notion of functional lateralization of the human brain, particularly the superiority of the left hemisphere in language processing [45]. Recent fMRI studies also show the essential role of the right side of the brain in language [46], which explains the formation of large community in the right hemisphere. Community #5 consists of more diverse nodes from both hemisphere suggesting its involvement in cross-hemisphere interaction. Interestingly, it comprises the key regions of language networks including middle-temporal-gyrus (MTG, both left and right), a major area involved in language processing, both comprehension and production. Community #5 also includes the thalamus (THA, both left and right) which plays a central role in synchronizing separate areas within linguistic processing [47], [48]. Fig. 8 shows the detected community structure for the motor task, where 18 communities are identified. These include 4 large communities (Community #1, #2, #4 and #5) and 14 singleton communities. Community #1 consists of major motor areas including the primary motor cortex (precentral gyrus (PreCG), both left and right) and supplementary motor areas (SMA). It also includes regions of parietal lobe which interacts with other regions such as motor cortex by integrating visual-motor information for movement control [49]. Community #2 mainly comprises frontal regions.

Given the estimated common community structure, we computed the time-dependent inter-module or inter-block connection probabilities (higher probability indicates higher density of edges) and estimated the state-based changes in the connectivity patterns between communities. Fig. 9 shows the estimated block connection probability matrices between four largest communities for story and math states of language



(a) Language task



(b) Motor task

Fig. 6. Tracking of regime changes in the inter-community connectivity of fMRI functional networks over 400 subjects for language and motor task experiments. (Top) Ground-truth task state time courses from experimental design. (Middle & Bottom) Dynamic state estimates by MS-SBM and K-means clustering.

task. We can see the networks exhibit non-purely assortative community structure mixed of assortative and core-periphery configurations. The communities of left and right hemispheres (#1 and #2) are assortative with denser connections within community of each hemispheres but sparser cross-hemisphere connections. These two segregated communities may engage in specialized information processing in language perception. Community #5 with nodes from both hemispheres is non-assortative in the form of core-periphery motif. It acts as a core-like community with strong intra-community connection density while projecting inter-community interactions with periphery-like communities (#1 and #2) with relatively sparsely connected nodes. This may suggest its role of information integration in language processing, transiently broadcasting information to or receive information from periphery across hemispheres. The connectivity between large commu-

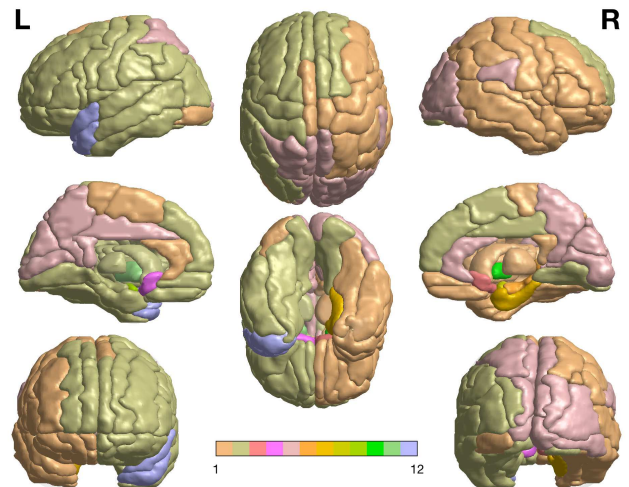


Fig. 7. Group-level brain community structure over 400 subjects detected from the language task fMRI based on multilayer modularity maximization. The 90 ROIs were color-coded according to their assigned communities.

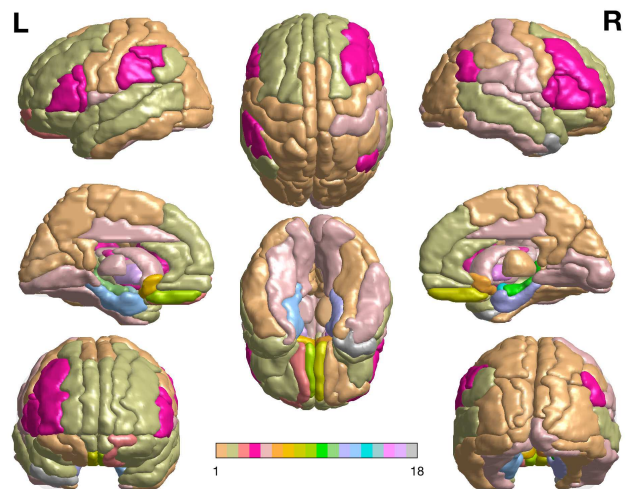


Fig. 8. Group-level brain community structure over 400 subjects detected from the motor task fMRI based on multilayer modularity maximization. The 90 ROIs were color-coded according to their assigned communities.

nities in the story and math tasks share similar patterns, partly due to the overlapping sensory and cognitive effort required in both tasks such as auditory and phonetic perception, syntactic analysis, attention and working memory. Nevertheless, slightly denser connection was elicited within the community #5 in story task, probably to facilitate more complex semantic processing when comprehending spoken narratives, compared to the non-semantic processes in the math task. The estimated connectivity matrices for the motor tasks in Fig. 10 also exhibit non-assortative community motif for all the six states. Community #1 serves as the core interacting with periphery communities #2 and #5. Communities #2 and #5 are less assortative with low within-community connection density.

The difference in the inter-community connectivity patterns across distinct states is more pronounced when including the singleton communities. Fig. 11 and Fig. 12 show interactions between all communities detected for the language and motor tasks, respectively. The links represent the averaged inter-block connection probabilities over subjects. We observed markedly

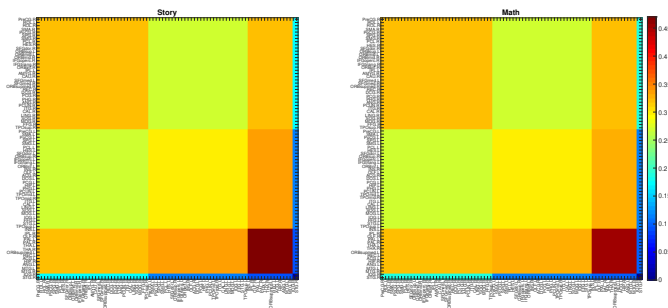


Fig. 9. Estimated median modular connection probability matrices between four largest communities for two states in the language tasks: story (left) and math (right).

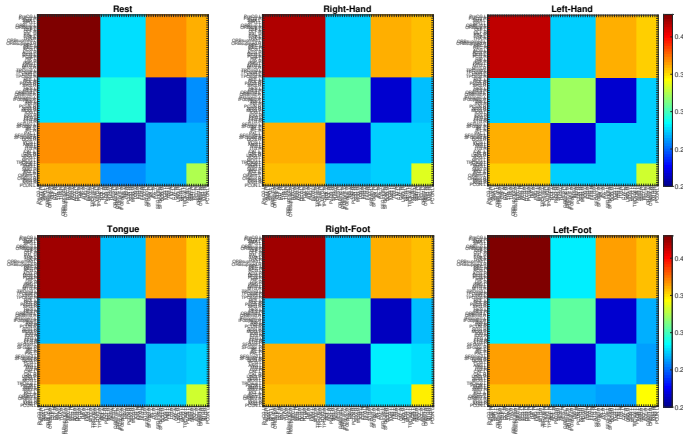


Fig. 10. Estimated median modular connection probability matrices between four largest communities for six states in the motor tasks.

distinct motifs of community interactions between the states in both tasks. In the language task, we see stronger between-community connectivity in the story task than the math. In the motor task, we found increase in connectivity within and between communities in the hand and foot movements compared to the resting state and tongue movement. Moreover, the left and right movement also exhibit distinct network configuration.

We evaluate the dynamic state estimation performance under subject-level and group-level community partitions, detected by the subject-specific and multi-subject Q_{\max} algorithms, respectively. We also compare the HMM and K-means clustering in tracking dynamic connectivity states. Fig. 13 plots the distributions of ARIs of estimated state sequences relative to changes of conditions in the experiments over 400 subjects. The higher ARIs for both tasks further confirm the results in Fig. 6 on the superiority of the proposed MSS-SBM over the K-means clustering for temporal shifts between distinct states of modular connectivity. Despite the advantage of subject-level community detection to account for inter-subject variability with varying numbers of communities and community organization for individual subjects, the use of common group-level community partition produces comparable results in ARIs for the dynamic state estimation. This implies existence of shared community structure among subjects and synchronous brain dynamics in response to the same tasks or stimuli, which may not apply to resting-state data.

VI. DISCUSSION

We developed a novel statistical framework based on a multilayer, Markov-switching SBM for identifying state-driven dynamic community structure in multi-subject brain functional networks. We first propose a multilayer SBM which is a generalization of existing dynamic SBM for single networks to an ensemble of networks, which provide a principled way of characterizing time-dependent community structure of brain networks for a group of subjects. The model allows brain nodes to share common community partition over multiple network layers formed by aggregating connectivity matrices of individual subjects, but the inter-community connection density may vary flexibly across layers (subjects) and time. By augmenting the multilayer SBM with a Markov-switching model to describe the temporal dynamics, it enables us to identify distinct, repeating states with respect to inter-community connectivity over time, without a priori assumption on the temporal locations of the transition between states. We further introduce the use of multilayer modularity maximization for estimating the latent block structure of the proposed MSS-SBM, which can uncover common community assignments in functional networks of many subjects simultaneously. This overcomes the problem of inconsistent mapping of community labels across subjects in the transitional subject-specific community detection.

Simulation results show the effectiveness of the proposed multilayer modularity maximization for recovery of common community structure in multilayer networks even when the network is sparse and the number of communities to be detected is large. When applied to two sets of HCP task-based fMRI data, our method detected more diverse community organization in addition to the typical assortative structure in brain networks, which is associated with language processing and motor functions. Even more notable is that our method was able to identify non-assortative community motifs such as the core-periphery structure. These types of network architecture engender more complex inter-community interactions that may allow the network to engage in a wider functional repertoire, e.g., integration of information across different brain regions in higher-order cognitive processes. For example, we found a bilateral core-like community in the language network that subserves an integrative function between periphery communities in the left and the right hemisphere during language comprehension. The proposed MSS-SBM also captures state-related dynamic re-configuration of inter-modular interactions in the brain networks, as modulated by the repetitive changes in task conditions over time course of experiment. It identified a set of putative network states with distinct profile of within and between-community connectivity that are differential between task conditions, such as left and right movements in the motor fMRI data.

Our method has produced findings that could lead to new sets of hypothesis about dynamic brain functional networks particularly the state-driven reconfiguration of the brain modular structure over time. Future work could investigate the behavioral relevance of the switching between states of network modularity, e.g., switching rate as a predictive of cognitive

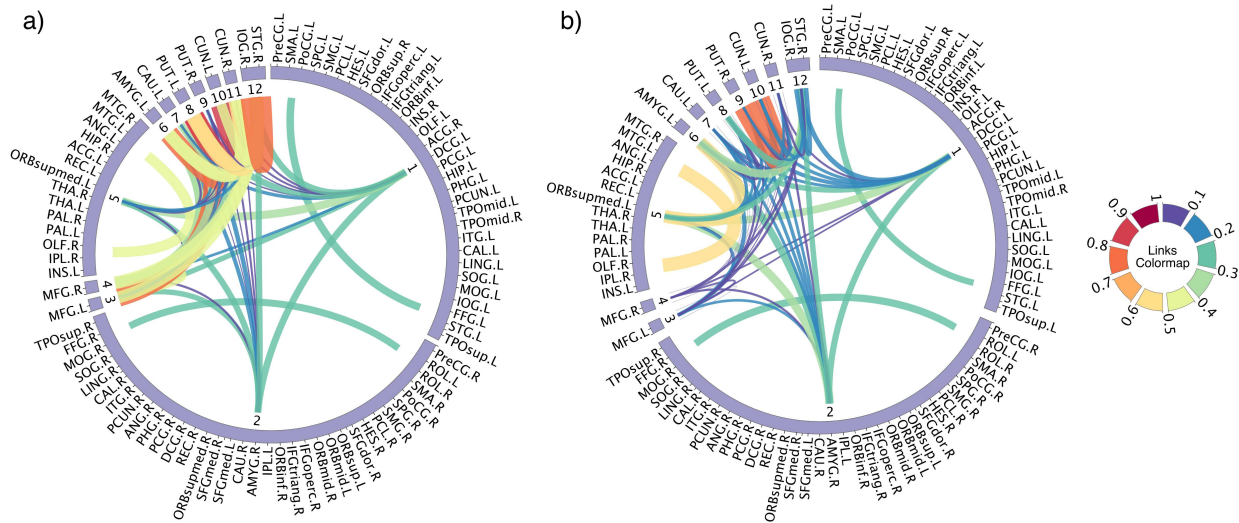


Fig. 11. Within and between-community connectivity for each state of the language task. (a) Story. (b) Math.

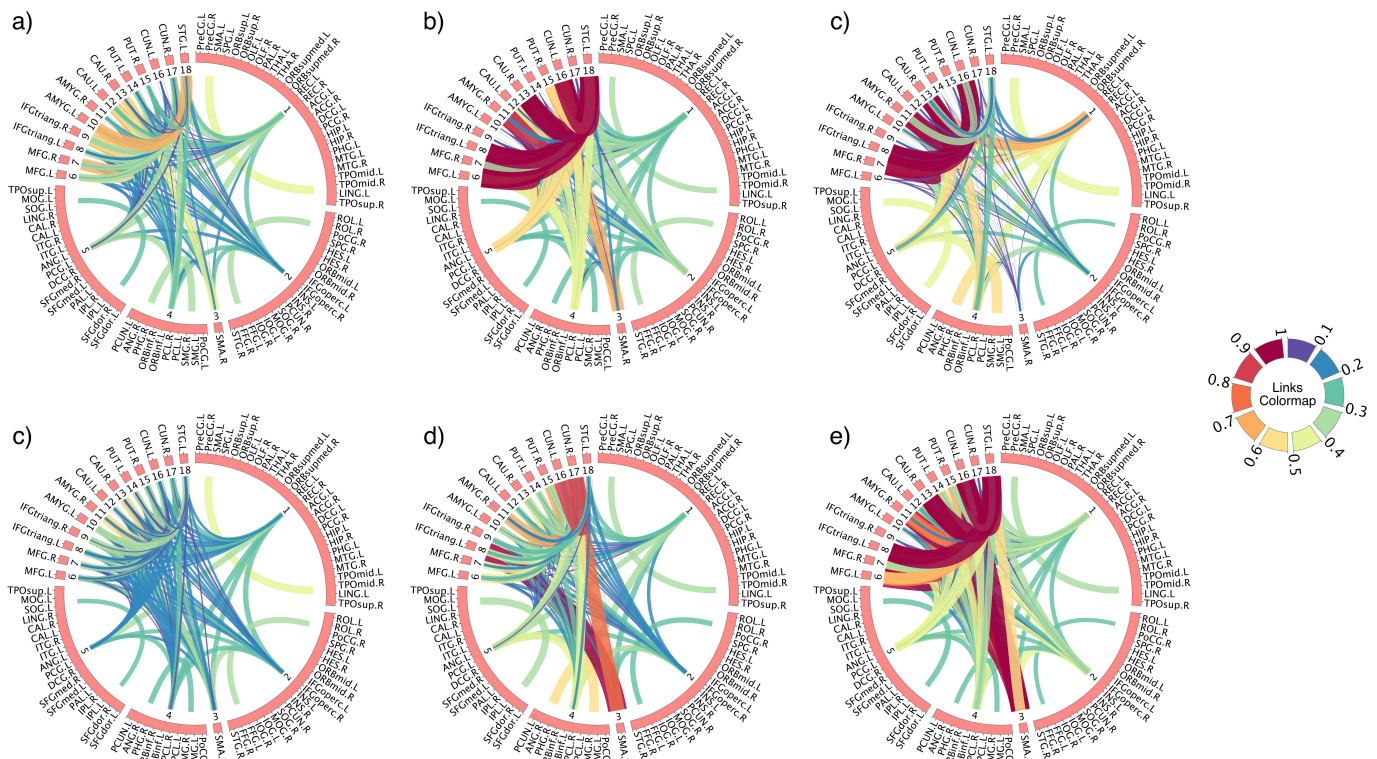


Fig. 12. Within and between-community connectivity for each state of the motor tasks. (a) Rest. (b) Right-hand. (c) Left-foot. (d) Tongue. (e) Left-hand. (f) Right-foot.

ability. Our current framework builds upon a basic SBM which assumes binary networks where edges carry no weights and identical degree distribution of each node. It can be extended to incorporate enhanced variants of SBM, such as the degree-corrected SBM [50] to allow for degree heterogeneity within communities, and weighted SBM [51] to handle weighted connectivity networks.

REFERENCES

- [1] E. Bullmore and O. Sporns, “Complex brain networks : Graph theoretical analysis of structural and functional systems,” *Nature Rev. Neurosci.*, vol. 10, pp. 186–198, 2009.
- [2] C. Chang and G. H. Glover, “Time-frequency dynamics of resting-state brain connectivity measured with fMRI,” *NeuroImage*, vol. 50, no. 1, pp. 81–98, mar 2010.
- [3] R. M. Hutchison, et al., “Dynamic functional connectivity: Promise, issues, and interpretations,” *NeuroImage*, vol. 80, pp. 360–378, 2013.
- [4] B. Rashid, et al., “Dynamic connectivity states estimated from resting fMRI Identify differences among schizophrenia, bipolar disorder, and healthy control subjects,” *Front. Hum. Neurosci.*, vol. 8, no. November, pp. 1–13, 2014.
- [5] V. L. Morgan, B. Abou-Khalil, and B. P. Rogers, “Evolution of functional connectivity of brain networks and their dynamic interaction in temporal lobe epilepsy,” *Brain Connectivity*, vol. 5, no. 1, pp. 35–44, 2014.
- [6] A. P. Baker, et al., “Fast transient networks in spontaneous human brain activity,” *eLife*, vol. 2014, no. 3, pp. 1–18, 2014.

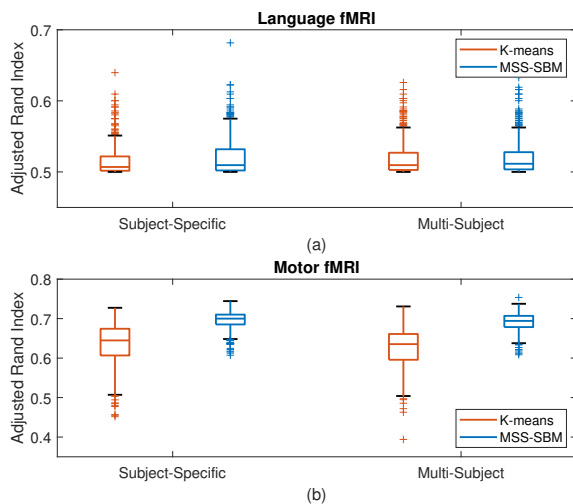


Fig. 13. Comparison of different community detection methods and temporal clustering methods in tracking the modular connectivity state dynamics in the language and motor tasks, as measured by ARI values of estimated state time courses relative to the experimental ground-truth over 400 subjects.

- [7] E. A. Allen, et al., “Tracking whole-brain connectivity dynamics in the resting state,” *Cereb. Cortex*, vol. 24, no. 3, pp. 663–676, 2012.
- [8] O. Sporns and R. F. Betzel, “Modular brain networks,” *Annu. Rev. Psychol.*, vol. 1, no. 67, pp. 613–640, 2016.
- [9] M. E. J. Newman and M. Girvan, “Finding and evaluating community structure in networks,” *Physical Rev. E*, vol. 69, no. 2, pp. 026113, feb 2004.
- [10] A. Clauset, M. E. Newman, and C. Moore, “Finding community structure in very large networks,” *Physical Rev. E*, vol. 70, no. 6, pp. 066111, 2004.
- [11] V. D. Blondel, et al., “Fast unfolding of communities in large networks,” *J. Statist. Mechanics: Theory and Experiment*, vol. 2008, no. 10, 2008.
- [12] K. Nowicki and T. A. B. Snijders, “Estimation and prediction for stochastic blockstructures,” *J. Amer. Stat. Assoc.*, vol. 96, no. 455, pp. 1077–1087, 2001.
- [13] R. F. Betzel, J. D. Medaglia, and D. S. Bassett, “Diversity of meso-scale architecture in human and non-human connectomes,” *Nat. Commun.*, vol. 9, no. 1, pp. 1–14, 2018.
- [14] P. J. Bickel and A. Chen, “A nonparametric view of network models and newman-girvan and other modularities,” *Proc. Natl. Acad. Sci. U.S.A.*, vol. 106, no. 50, pp. 21068–21073, 2009.
- [15] Y. Chen, et al., “Convexified modularity maximization for degree-corrected stochastic block models,” *Ann. Statist.*, vol. 46, no. 4, pp. 1573–1602, 2018.
- [16] D. S. Bassett, et al., “Dynamic reconfiguration of human brain networks during learning,” *Proc. Natl. Acad. Sci. U.S.A.*, vol. 108, no. 18, pp. 7641–7646, 2011.
- [17] M. Pedersen, et al., “Multilayer network switching rate predicts brain performance,” *Proc. Natl. Acad. Sci. U.S.A.*, vol. 115, no. 52, pp. 13376–13381, 2018.
- [18] D. M. Pavlovic, et al., “Stochastic blockmodeling of the modules and core of the *Caenorhabditis elegans* connectome,” *PLoS ONE*, vol. 9, no. 7, 2014.
- [19] K. S. Xu and A. O. Hero, “Dynamic stochastic blockmodels for time-evolving social networks,” *IEEE J. Sel. Topics Signal Process.*, vol. 8, no. 4, pp. 552–562, 2014.
- [20] C. Matias and V. Miele, “Statistical clustering of temporal networks through a dynamic stochastic block model,” *J. Royal Stat. Society: Series B*, vol. 79, no. 4, pp. 1119–1141, 2017.
- [21] E. M. Gordon, et al., “Individual variability of the system-level organization of the human brain,” *Cerebral Cortex*, vol. 27, no. 1, pp. 386–399, 2017.
- [22] P. J. Mucha, et al., “Community structure in time-dependent, multiscale, and multiplex networks,” *Science*, vol. 328, no. 5980, pp. 876–878, 2010.
- [23] R. F. Betzel, et al., “The community structure of functional brain networks exhibits scale-specific patterns of inter-and intra-subject variability,” *NeuroImage*, 2019, In press.
- [24] L. F. Robinson, L. Y. Atlas, and T. D. Wager, “Dynamic functional connectivity using state-based dynamic community structure: Method and application to opioid analgesia,” *NeuroImage*, vol. 108, pp. 274–291, mar 2015.
- [25] D. M. Pavlovic, et al., “Multi-subject stochastic blockmodels for adaptive analysis of individual differences in human brain network cluster structure,” *bioRxiv preprint*, 2019.
- [26] S. B. Samdin, C.-M. Ting, and H. Ombao, “Detecting state changes in community structure of functional brain networks using a markov-switching stochastic block model,” in *16th IEEE Int. Symp. Biomed. Imaging*, 2019.
- [27] E. T. Bullmore and D. S. Bassett, “Brain graphs: Graphical models of the human brain connectome,” *Annual Rev. Clinical Psychology*, vol. 7, pp. 113–140, 2011.
- [28] P. A. Bandettini, et al., “Tracking ongoing cognition in individuals using brief, whole-brain functional connectivity patterns,” *Proc. Natl. Acad. Sci. U.S.A.*, vol. 112, no. 28, pp. 8762–8767, 2015.
- [29] S. B. Samdin, et al., “A unified estimation framework for state-related changes in effective brain connectivity,” *IEEE Trans. Biomed. Eng.*, vol. 64, no. 4, pp. 844–858, 2017.
- [30] C. M. Ting, et al., “Estimating dynamic connectivity states in fMRI using regime-switching factor models,” *IEEE Trans. Med. Imaging*, vol. 37, no. 4, pp. 1011–1023, 2018.
- [31] M. E. J. Newman, “Modularity and community structure in networks,” *Proc. Natl. Acad. Sci. U.S.A.*, vol. 103, no. 23, pp. 8577–8582, 2006.
- [32] D. S. Bassett, et al., “Robust detection of dynamic community structure in networks,” *Chaos*, vol. 23, no. 1, 2013.
- [33] A. N. Khambhati, et al., “Modeling and interpreting mesoscale network dynamics,” *NeuroImage*, vol. 180, no. June 2017, pp. 337–349, 2018.
- [34] K. Rohe, S. Chatterjee, and B. Yu, “Spectral clustering and the high-dimensional stochastic blockmodel,” *Ann. Statist.*, vol. 39, no. 4, pp. 1878–1915, 2011.
- [35] L. E. Jing and A. Rinaldo, “Consistency of spectral clustering in stochastic block models,” *Ann. Statist.*, vol. 43, no. 1, pp. 215–237, 2015.
- [36] L. Rabiner, “A tutorial on hidden Markov models and selected applications in speech recognition,” *Proc. IEEE*, vol. 77, no. 2, pp. 257–286, 1989.
- [37] Y. Zhao, et al., “Consistency of community detection in networks under degree-corrected stochastic block models,” *Ann. Statist.*, vol. 40, no. 4, pp. 2266–2292, 2012.
- [38] F. Krzakala, et al., “Spectral redemption in clustering sparse networks,” *Proc. Natl. Acad. Sci. U.S.A.*, vol. 110, no. 52, pp. 20935–20940, 2013.
- [39] D. M. Barch, et al., “Function in the human connectome: Task-fMRI and individual differences in behavior,” *NeuroImage*, vol. 80, pp. 169–189, oct 2013.
- [40] J. R. Binder, et al., “Mapping anterior temporal lobe language areas with fMRI: A multicenter normative study,” *NeuroImage*, vol. 54, no. 2, pp. 1465–1475, Jan 2011.
- [41] M. F. Glasser, et al., “The minimal preprocessing pipelines for the human connectome project,” *NeuroImage*, vol. 80, pp. 105–124, 2013.
- [42] R. Schmidt, et al., “Proportional thresholding in resting-state fMRI functional connectivity networks and consequences for patient-control connectome studies: Issues and recommendations,” *NeuroImage*, vol. 152, no. February, pp. 437–449, 2017.
- [43] L. G. S. Jeub, et al., “A generalized Louvain method for community detection implemented in MATLAB,” 2017.
- [44] D. S. Bassett, et al., “Task-based core-periphery organization of human brain dynamics,” *PLoS Computational Biology*, vol. 9, no. 9, 2013.
- [45] J. A. Frost, et al., “Language processing is strongly left lateralized in both sexes: Evidence from functional MRI,” *Brain*, vol. 122, no. 2, pp. 199–208, 1999.
- [46] A. M. Muller and M. Meyer, “Language in the brain at rest: New insights from resting state data and graph theoretical analysis,” *Front. Hum. Neurosci.*, vol. 8, pp. 228, 2014.
- [47] M. D. Johnson and G. A. Ojemann, “The role of the human thalamus in language and memory: Evidence from electrophysiological studies,” *Brain and cognition*, vol. 42, no. 2, pp. 218–230, 2000.
- [48] F. Klostermann, “Functional roles of the thalamus for language capacities,” *Front. Syst. Neurosci.*, vol. 7, pp. 32, 2013.
- [49] L. Fogassi and G. Luppino, “Motor functions of the parietal lobe,” *Current Opinion in Neurobiology*, vol. 15, no. 6, pp. 626–631, 2005.
- [50] B. Karrer and M. E. Newman, “Stochastic blockmodels and community structure in networks,” *Physical Rev. E*, vol. 83, no. 1, pp. 016107, 2011.
- [51] C. Aicher, A. Z. Jacobs, and A. Clauset, “Learning latent block structure in weighted networks,” *J. Complex Networks*, vol. 3, no. 2, pp. 221–248, 2014.